

# A Generic Unified Model for the IceCube Neutrinos and the Ultra-high Energy Cosmic Rays in the Photomeson Production Scenario

---

**Shigeru Yoshida**<sup>\*†</sup>

*Department of Physics, Graduate School of Science, Chiba University, Chiba 263-8522, Japan*  
*E-mail: [syoshida@hepburn.s.chiba-u.ac.jp](mailto:syoshida@hepburn.s.chiba-u.ac.jp)*

**Kohta Murase**

*Department of Physics & Astronomy; Institute for Gravitation and Cosmology, The Pennsylvania State University, University Park, PA 16802, USA*  
*and*  
*Yukawa Institute for Theoretical Physics, Kyoto University, Kyoto, Kyoto 606-8502, Japan*  
*E-mail: [murase@psu.edu](mailto:murase@psu.edu)*

We construct a generic unified model of sources to account observations of ultra-high energy cosmic rays at  $\gtrsim 10^{19}$  eV as well as high energy neutrinos above 100 TeV in a framework of photomeson interactions. The mildly efficient in-situ production of  $\gtrsim 100$  TeV neutrinos with  $0.1 \lesssim \tau_{\gamma p} \lesssim 0.4$  must be realized in a source environment to accelerate cosmic rays to ultra-high energies. The measured fluxes of cosmic rays and neutrinos set the bound on the source luminosity and the emission rate. Tidal disruption events (TDEs) and low-luminosity GRBs are consistent with the present requirements if the Lorentz bulk factor of plasma and the equipartition parameters for cosmic rays and magnetic field are appropriately selected.

*36th International Cosmic Ray Conference -ICRC2019-  
July 24th - August 1st, 2019  
Madison, WI, U.S.A.*

---

\*Speaker.

†A footnote may follow.

## 1. Introduction

The detection of a bulk of cosmic neutrinos in the energy range from  $\sim 10$  TeV to  $\sim$  PeV by the IceCube Neutrino Observatory [1, 2] exposed very interesting questions. The observed energy flux of high energy neutrinos appears comparable with that of ultra-high energy cosmic rays (UHECRs) at  $\gtrsim 10^{19}$  eV. The origin of high energy neutrinos are associated with UHECR sources? The both neutrino and UHECR fluxes are consequences of yet-unknown common astrophysical phenomena? Several studies to probe these possibilities have been conducted in the literature, mainly in the framework of hadronuclear ( $pp$ ) collisions inside a cosmic ray reservoir – Starburst galaxies, black-hole jets embedded in a cluster of galaxies, and so on [3]. High energy neutrinos can be produced, however, also by photomeson interactions ( $p\gamma$ ) in the cosmic ray emitters.  $p\gamma$  collisions may occur simultaneously or successively to acceleration of cosmic rays. If acceleration power is large enough, it is indeed possible to emit both  $\gtrsim 100$  TeV neutrinos and UHECRs.

In this paper, we present a generic unified model for the neutrinos with energies greater than 100 TeV and UHECRs in the photomeson production scheme. The neutrino background flux is estimated analytically with parameters to characterize sources such as the photon luminosity and the source number density. The UHECR nucleon flux is also estimated analytically taking into account their collisions with background photons in the intergalactic space. We also derive the requirements of being capable to accelerate cosmic ray protons to ultra-high energies and transform them to the criteria of the parameters relevant to the high energy neutrino emissions like the optical depth of  $p\gamma$  interactions. The estimated fluxes of neutrinos and UHECRs from sources satisfying these criteria are compared with the measured flux at 100 TeV  $\lesssim E_\nu \lesssim 10$  PeV and its upperlimit at  $E_\nu \gtrsim 100$  PeV by IceCube, as well as the measurement of UHECRs at  $10^{19}$  eV. The resultant constraints on the parameters regarding general source characteristics are presented. We finally describe a case study for specific astronomical objects such as low-luminosity GRBs.

## 2. Source modelling

For a reference energy of UHECR protons  $E_0^s$  at a source, the typical energy of target photons is determined by the  $\Delta$  resonance feature of the photomeson interactions. The relation is given by

$$E'_{\gamma,\text{ref}} = \frac{(s_R - m_p^2) \Gamma}{4 E_0^s} \quad (2.1)$$

where  $s_R \simeq (1.23 \text{ GeV})^2$  is the square of invariant mass of the  $p\gamma$  collisions at the  $\Delta$  resonance. Primed (') characters represent quantities measured in the rest frame of plasma with the Lorentz bulk factor  $\Gamma$ . The  $p\gamma$  optical depth  $\tau_{\gamma p} \equiv d'/\lambda'_{\gamma p}$  characterizes the neutrino production efficiency at a source. The size of the site where  $p\gamma$  collisions occur,  $d'$ , is comparable to  $R/\Gamma$ , where  $R$  is a distance of the  $p\gamma$  collision spot from the central core of a neutrino source. When the target photon spectrum is approximated to be represented by a power law  $\sim (E'_\gamma)^{-\gamma}$  around  $E'_{\gamma,\text{ref}}$ , the formulation in Ref. [5] then gives  $\tau_{\gamma p} = \tau_0^{\gamma p} (E_p/E_0^s)^{\gamma-1}$  with

$$\tau_0^{\gamma p} = \begin{cases} 8 \frac{L'_\gamma}{4\pi R c \Gamma^2} \frac{\gamma-2}{\gamma+1} (s_R - m_p^2)^{\gamma-2} \frac{E_0^s}{x_d^{-\gamma+2} - x_u^{-\gamma+2}} \int ds \sigma_{\gamma p}(s) (s - m_p^2)^{-\gamma} & \gamma \neq 2 \\ 8 \frac{L'_\gamma}{4\pi R c \Gamma^2} \frac{1}{3} (s_R - m_p^2)^{\gamma-2} \frac{E_0^s}{\ln\left(\frac{E_\gamma^{\text{max}}}{E_\gamma^{\text{min}}}\right)} \int ds \sigma_{\gamma p}(s) (s - m_p^2)^{-\gamma} & \gamma = 2. \end{cases} \quad (2.2)$$

Here photons in the energy region of  $E_\gamma^{\min} \leq E'_\gamma \leq E_\gamma^{\max}$  whose center is  $E'_{\gamma,\text{ref}}$  are involved with the photomeson production. The two parameters  $x_d = (E_\gamma^{\min}/E'_{\gamma,\text{ref}})$  and  $x_u = (E_\gamma^{\max}/E'_{\gamma,\text{ref}})$  represents the boundary of this energy belt. We remark that  $\tau_0^{\gamma p} \sim 1/\Gamma^2$  for a given comoving photon luminosity  $L'_\gamma = L_\gamma/\Gamma^2$ . Also note that there is an inexplicit  $\Gamma$  dependence via Eq. (2.1), implying that the optical depth is always defined in the density of photons at energy of  $E'_{\gamma,\text{ref}}$ , as this is the representative target photon energy in the photopion production for a UHECR proton with energy of  $E_0^s$ . In this parameterization scheme, the reference proton energy  $E_0^s$  is fixed and the optical depth  $\tau_0^{\gamma p}$  is always defined at  $E'_{\gamma,\text{ref}}$  given by Eq. 2.1. Throughout this report, we set  $E_p^{\min} = E_0^s = 10$  PeV.

The magnetic energy density in the shock rest frame,  $U'_B$ , is given as  $U'_B = \xi_B L'_\gamma / 4\pi R^2 c$  where  $\xi_B$  is the equipartition parameter. A given radius of the  $p\gamma$  interaction site,  $R$ , appearing in Eq. (2.2), is thus connected to the magnetic field strength via this relation above. As  $R \sim L'_\gamma / \tau_0^{\gamma p} \Gamma^2$  and  $U'_B \sim L'_\gamma / R^2$ , the magnetic field  $B' \sim \Gamma^2 \tau_0^{\gamma p} / \sqrt{L'_\gamma}$ . The synchrotron cooling of UHECR protons limits the UHECR acceleration capability. Secondary muons and pions produced by the photomeson interactions also lose their energies via the synchrotron radiation, which results in suppression of the neutrino flux. Requiring  $t_{\pi,\mu}^{\text{sync}} / \tau_{\pi,\mu} \leq 1$ , the cutoff energy of the neutrino flux due to the synchrotron cooling goes  $\sim \Gamma / \sqrt{U'_B} \sim \Gamma R / \sqrt{\xi_B L'_\gamma}$ . As the optical depth  $\tau_0^{\gamma p}$  scales to  $\sim L'_\gamma / R \Gamma^2$ , we find the cutoff energy scales to  $\sqrt{L'_\gamma} / \sqrt{\xi_B \Gamma} \tau_0^{\gamma p}$ . Thus the upperlimit of the neutrino flux in the energy region beyond 10 PeV by IceCube [4] constrains  $L'_\gamma$  and  $\tau_0^{\gamma p}$ .

Fluxes of high energy neutrinos for a given optical depth  $\tau_0^{\gamma p}$  are analytically calculated in Ref. [5]. We employ their formulations with minor modifications to take the synchrotron cooling into account. The source evolution is assumed to compatible with the star formation rate, which is consistent with the constraints from the Extremely-high energy (EHE) analysis by IceCube [6]. The spectrum of UHECR protons after their propagation in the intergalactic space to reach to the earth is calculated by the similar analytical technique. The details will be published elsewhere. The cosmic ray luminosity in the energy region above  $E_0^s (= 10$  PeV),  $L_{\text{CR}}$ , is considered here to define the power channeling into cosmic rays here. For an UHECR fluence emitted from a source  $dN_{\text{CR}}/dE_p^s = \kappa_{\text{CR}} (E_p^s/E_0^s)^{-\alpha}$ , we calculate  $L_{\text{CR}}$  as  $L_{\text{CR}} = \int_{E_0^s} dE_p^s E_p^s dN_{\text{CR}}/dE_p^s$ . The UHECR and the photon emissions are connected via the CR loading factor  $\xi_{\text{CR}}$  by  $L_{\text{CR}} = \xi_{\text{CR}} L_\gamma$ .

Introducing the comoving number density of sources in the local universe,  $n_0 = \rho_0 \Delta T$ , where  $\rho_0$  and  $\Delta T$  are the rate density and the time duration of transient phenomena at sources, both the UHECR and the neutrino diffuse fluxes scale to  $\sim n_0 \kappa_{\text{CR}} \sim n_0 \xi_{\text{CR}} L_\gamma \sim n_0 \xi_{\text{CR}} L'_\gamma \Gamma^2$ . It is convenient to introduce the *inclusive* source number density defined as

$$\mathcal{N}_\Gamma \equiv n_0 \xi_{\text{CR}} \Gamma^2. \quad (2.3)$$

Then the UHECR and neutrino intensities are proportional to  $\mathcal{N}_\Gamma$  for a given comoving photon luminosity  $L'_\gamma$ .

Figure 1 shows an example of the UHECR and neutrino fluxes derived by the present generic model. The star-formation-like evolution is assumed. This realization of the fluxes displayed in Figure 1 belongs to a scenario consistent with the UHECR and IceCube data. We discuss the allowed parameter space in the next section. Note that the  $1/\Gamma$  dependence of the neutrino cutoff energy due to the muon/pion synchrotron loss is also observed in this plot.

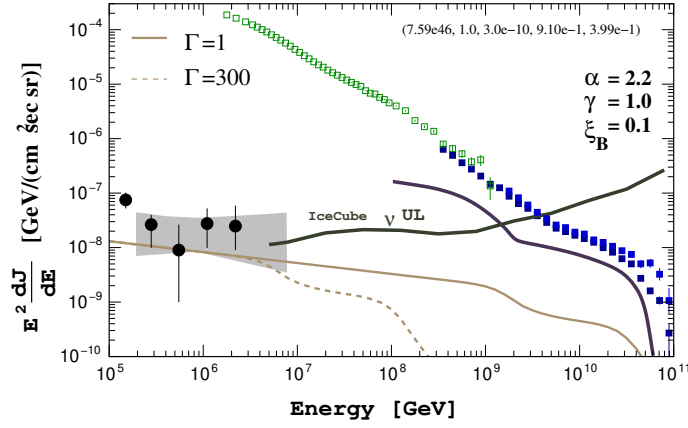


**Figure 1:** An example of the UHECR nucleon and the neutrino fluxes from UHECR sources calculated by the present formulation. A case of  $\alpha = 2.2$ ,  $\gamma = 1.0$ ,  $\xi_B = 0.1$  is shown. The star formation rate-like evolution is assumed. The comoving  $L'_\gamma$  is set to  $7.6 \times 10^{46}$  erg/s and the inclusive source number density  $\mathcal{N}_\Gamma$  (Eq. 2.3) is  $3 \times 10^{-10}$  Mpc $^{-3}$ . The optical depth  $\tau_0^{\gamma p}$  is 0.40 in this particular example, which gives the magnetic field of  $B' = 0.91\Gamma^2$  Gauss with  $\xi_B = 0.1$ . The black points are the IceCube neutrino measurements [7] and the shade region represents the flux space consistent with the IceCube diffuse  $\nu_\mu$  data [2]. The solid curve labeled by (IceCube  $\nu$  UL) is the differential EHE bound by IceCube [4]. The cosmic ray data measured by PAO [8] and TA [9] is also displayed.

The present generic model has been constructed in such way that for a given  $L'_\gamma$ ,  $\mathcal{N}_\Gamma$  and  $\Gamma$ , the  $p\gamma$  interaction site radius  $R$  can be varied to realize various  $\tau_0^{\gamma p}$  and  $U_B$  (assuming values of the equipartition parameters  $\xi_{CR}$  and  $\xi_B$ ). Thus the explicit independent parameters are  $L'_\gamma$ ,  $\mathcal{N}_\Gamma$ ,  $\Gamma$ , and  $\tau_0^{\gamma p}$  using Eq. (2.2).

### 3. Required conditions for UHECR and neutrino sources

For sources to be responsible for UHECR emission, the cosmic ray acceleration time scale,  $t_p^{\text{acc}}$ , must be faster than the dynamical time scale  $t_p^{\text{dyn}} \sim R/c\Gamma$ . As  $(t_p^{\text{acc}})^{-1} = c\Gamma eB'E_p^{-1}$ , this condition is transformed to the well known formula [10],

$$L'_\gamma \geq \frac{1}{2} \xi_B^{-1} c \left( \frac{E_p^{\text{max}}}{e} \right)^2 = 6.7 \times 10^{45} \xi_B^{-1} \left( \frac{E_p^{\text{max}}}{2.0 \times 10^{11} \text{GeV}} \right)^2 \text{ erg/s} \quad (3.1)$$

UHECRs must be accelerated before cooling by the Synchrotron radiation, *i.e.*,  $t_p^{\text{acc}} \leq t_p^{\text{sync}}$ . With Eq.( 2.2), it leads to the bound on  $\sqrt{L'_\gamma/\xi_B/\tau_0^{\gamma p}}$ :

$$\frac{6e}{\sigma_T \tau_0^{\gamma p}} \frac{\gamma-2}{\gamma+1} \sqrt{2 \frac{L'_\gamma}{\xi_B c} \left( \frac{m_p}{m_e} \right)^2} (s_R - m_p^2)^{\gamma-2} \frac{E_o^s}{x_d^{-\gamma+2} - x_u^{-\gamma+2}} \int ds \sigma_{\gamma p}(s) (s - m_p^2)^{-\gamma} \geq \left( \frac{E_p^{\text{max}}}{m_p c^2} \right)^2. \quad (3.2)$$

Here  $E_p^{\text{max}} = 2 \times 10^{11}$  GeV is the maximal energy of UHECR protons accelerated at sources.

In order that UHECRs can be escaped from sources before losing their energies by the synchrotron cooling, the dynamical time scale  $t_p^{\text{dyn}}$  must be faster than  $t_p^{\text{sync}}$ . Note that the escape time scale is comparable to the dynamical scale in a relativistic environment of UHECR acceleration

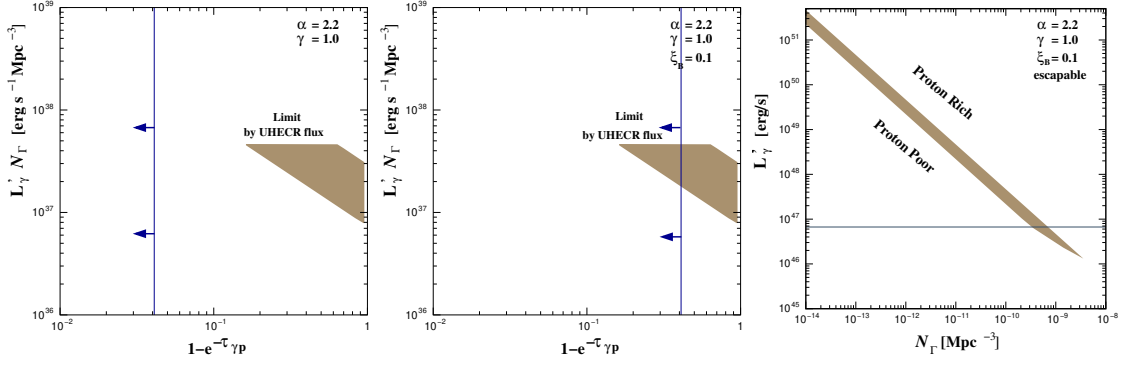


**Figure 2:** The obtained constraints on the source characteristics when  $\alpha = 2.2$  and  $\gamma = 1.0$ . (Left) The allowed region on the parameter space of  $L'_\gamma \mathcal{N}_\Gamma$  and the dumping factor  $1 - e^{-\tau_0^{\gamma p}}$  for  $\xi_B = 1.0$ . The vertical line represents the bound on  $\tau_0^{\gamma p}$  by the UHECR escape condition, Eq. (3.3). (Center) Same as the left plot, but  $\xi_B = 0.1$ . (Right) The allowed region on the plane of  $L'_\gamma$  and  $\mathcal{N}_\Gamma$ . The horizontal line shows the condition of  $t_p^{\text{acc}} \leq t_p^{\text{dyn}}$ , Eq. (3.1).

site we currently consider. With the optical depth formula, Eq. (2.2), we can obtain the condition on  $\tau_0^{\gamma p}$  to meet this requirement, without explicitly depending on  $L'_\gamma$  and  $\Gamma$ :

$$\begin{aligned} \tau_0^{\gamma p} &\leq \frac{6}{\xi_B \sigma_T} \frac{\gamma - 2}{\gamma + 1} \left( \frac{m_p}{m_e} \right)^2 \left( \frac{E_p^{\text{max}}}{m_p c^2} \right)^{-1} \frac{E_0^s m_p c^2}{x_d^{-\gamma+2} - x_u^{-\gamma+2}} (s_R - m_p^2)^{\gamma-2} \int ds \sigma_{\gamma p}(s) (s - m_p^2)^{-\gamma} \\ &\lesssim 4.1 \times 10^{-2} \left( \frac{E_p^{\text{max}}}{2 \times 10^{11} \text{ GeV}} \right)^{-1} \xi_B^{-1} \end{aligned} \quad (3.3)$$

The criteria of the resultant fluxes of neutrinos and UHECRs are: (a) The integral UHECR proton flux above 10 EeV,  $\int_{10 \text{ EeV}} dE_p dJ_{\text{CR}}/dE_p$ , is below the measurement by Auger,  $8.5 \times 10^{-19}$  /cm<sup>2</sup> sec sr [8]. (b) The neutrino flux intensity at 100 TeV and the spectral power law index are within the 99 % C.L. range obtained by the diffuse  $\nu_\mu$  data measured by IceCube [2]. (c) The all flavor neutrino flux at 100 PeV is below  $2 \times 10^{-8}$  GeV/cm<sup>2</sup> sec sr, the limit obtained by the IceCube EHE analysis [4]. (d) The neutrino flux at 6 PeV is above  $2 \times 10^{-9}$  GeV/cm<sup>2</sup> sec sr, as IceCube detected a 6 PeV  $\bar{\nu}_e$  [4].

#### 4. Results

Figure 2 displays the constraints for the spectral power law index of UHECRs  $\alpha = 2.2$  and that of the target photons  $\gamma = 1$ . As the neutrino spectrum follows  $\sim E_\nu^{-(\alpha-\gamma+1)} \sim E_\nu^{-2.2}$ , they are a representative case of a relatively hard neutrino flux. The optical depth  $\tau_0^{\gamma p} \gtrsim 0.1$  is required as a consequence of the IceCube neutrino energy flux being compatible with UHECR flux. As seen in Figure 1, margins to vary fluxes of neutrinos to be consistent with both the neutrinos and UHECRs are really tight when the primary UHECR spectrum is as hard as  $\alpha \lesssim 2.2$ . Since  $L'_\gamma \mathcal{N}_\Gamma \sim n_0 \kappa_{\text{CR}}$ , the range of the multiplication  $L'_\gamma \mathcal{N}_\Gamma$  is bounded by the UHECR flux and the IceCube neutrino flux connected by the optical depth  $\tau_0^{\gamma p}$ . This is an expanded way of presenting the bounds leading to the frequently referred Waxman-Bahcall limit [11]. The tight constraint is also consistent with the results in Ref. [5]. However, the UHECR escape condition, Eq. (3.3), prevents such large optical depths unless the magnetic field is weaker than expected from the equipartition condition  $\xi_B = 1$ .

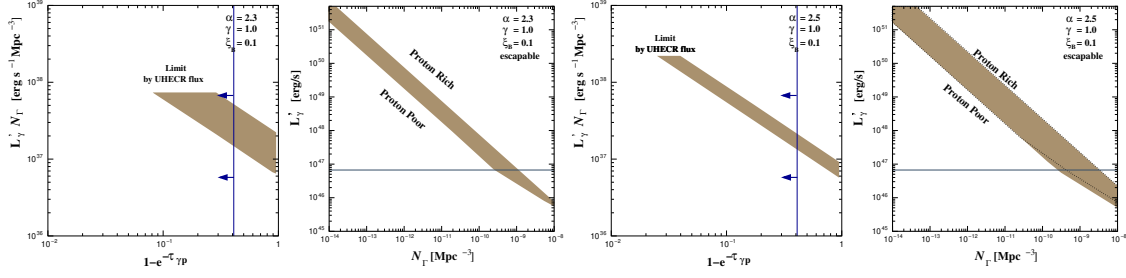


**Figure 3:** Same as Figure 2, but for  $\alpha = 2.3$  (left and middle left panels) and  $\alpha = 2.5$  (middle right and right panels).  $\xi_B = 0.1$  is assumed.

Relaxing the criteria involving the proton synchrotron cooling by setting  $\xi_B \sim 0.1$  can bring an allowed space of the parameters,  $L'_\gamma \mathcal{N}_\Gamma$  and the optical depth  $\tau_0^{\gamma p}$ . We found that the cases of even harder UHECR source spectrum, *i.e.*,  $\alpha \lesssim 2.1$  is nearly excluded for the reasonable range of magnetic field strengths expected by  $\xi_B \gtrsim 0.1$ .

As seen in Figure 3, a larger region of the parameter space is allowed when UHECR source spectrum is softer. We should remark, however, that the domain of  $L'_\gamma \mathcal{N}_\Gamma \gg 10^{37}$  erg/s Mpc<sup>3</sup> apparently allowed in case of  $\alpha = 2.5$  is not realistic as no such luminous and highly populated sources are known to exist in the universe.

Although the case of the hard UHECR spectrum, *i.e.*,  $\alpha \lesssim 2.1$  is nearly ruled out, a scenario predicting hard *neutrino* spectrum emission is still possible if the target photon spectrum is softer such as  $\gamma \gtrsim 1.3$ . The left and center panels in Figure 4 illustrates how the relevant parameter space is constrained in such cases. The hard neutrino spectrum extending well beyond 100 PeV can be excluded by the EHE flux limit [4]. A possible neutrino flux suppression due to the synchrotron cooling could avoid the rather strong constraints. As a consequence, substantially large  $\Gamma$  is required in the scenario with  $\gamma \gtrsim 1.3$ . This  $\Gamma$  dependence is shown in the right panel of Figure 4 displaying the allowed space on the plane of  $\alpha$  and  $\Gamma$  for various values of the photon spectral

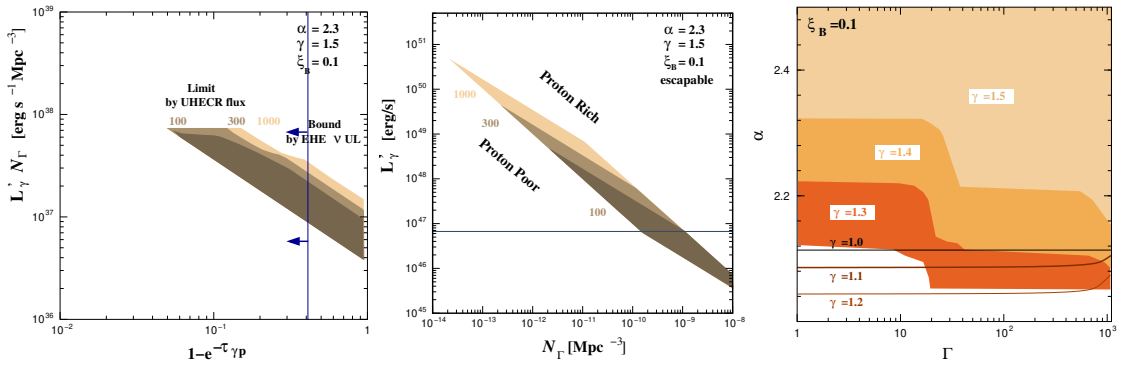


**Figure 4:** (Left and center) The obtained constraints on the source characteristics when  $\alpha = 2.3$ ,  $\gamma = 1.5$ , and  $\xi_B = 0.1$ .  $\Gamma \gtrsim 30$  is required to avoid being excluded by the IceCube EHE limit of the neutrino flux for  $E_\nu \geq 100$  PeV. Here the cases of  $\Gamma = 100, 300$ , and  $1000$  are shown by various color patches, respectively. (Right) The allowed region on the plane of  $\alpha$  and  $\Gamma$ . The regions for  $\gamma = 1.4$  and  $\gamma = 1.3$  are under-laid beneath the region of  $\gamma = 1.5$  for display purposes. The cases of  $\gamma = 1.0, 1.1$ , and  $1.2$  are shown by the solid curve. The region above each of the lines are allowed, respectively.

power law index  $\gamma$ . Less relativistic plasma flow like  $\Gamma \lesssim 20$  is excluded for  $\gamma \gtrsim 1.3$ .

## 5. Discussions

Our results are general and applicable to different types of  $p\gamma$  neutrino sources. Here we discuss possible classes of candidate sources that can satisfy the requirements for the unification scenario. The energy budget of different classes of steady and transient sources are summarized in Ref. [12].

Blazars, which are active galactic nuclei whose jets point to us, have been considered as promising cosmic-ray accelerators and high-energy neutrino emitters. The local source densities inferred from gamma-ray observations are  $n_0 \sim 10^{-7} \text{ Mpc}^{-3}$  for BL Lac objects and  $n_0 \sim 10^{-9} \text{ Mpc}^{-3}$ , respectively [13]. The bolometric luminosity of radiation from jets typical lies in  $L_\gamma \sim 10^{44} - 10^{48} \text{ erg s}^{-1}$ , implying comoving luminosities of  $L'_\gamma \sim 10^{43} - 10^{47} \text{ erg s}^{-1}$  with  $\Gamma \sim 3$ . Thus, blazars can in principle satisfy the requirements shown in Figures 2, 3, 4. However, an issue is that the observed photon spectral index for the relevant energy range is  $\gamma \sim 2 - 3$ , which predicts a hard neutrino spectrum in the standard scenario [14]. While we do not exclude blazars as a possible source class for the unified scenario, a new source model beyond the one-zone leptonic scenario would need to be constructed.

Tidal disruption events (TDEs) are attributed to the disruption of a star by a supermassive or intermediate mass black hole. A fraction of the TDEs are accompanied by powerful jets with  $L_\gamma \sim 10^{47} - 10^{48} \text{ erg s}^{-1}$  or  $L'_\gamma \sim 10^{46} - 10^{47} (\Gamma/3)^{-2} \text{ erg s}^{-1}$  [15], and they have also been suggested as the sources of UHECRs [16]. The rate density of TDEs like Sw J1644+57 is  $\rho_0 \sim 3 \times 10^{-11} \text{ Mpc}^{-3} \text{ yr}^{-1}$  [15] and the duration is  $\Delta T \sim 10^6 \text{ s}$ , implying that  $n_0 \sim 10^{-12} \text{ Mpc}^{-3}$  and  $\mathcal{N}_\Gamma \sim 5 \times 10^{-10} (\xi_{\text{CR}}/50)(\Gamma/3)^2 \text{ Mpc}^{-3}$ . Thus jetted TDEs can in principle satisfy the required constraints, which is consistent with the model of Ref. [17]. However, different analyses including multiplet limits and the analysis on Sw J1644+57 have excluded them as the main sources of IceCube neutrinos [18].

High-luminosity GRBs are among the most popular candidate sources of UHECRs [19]. The rate density is  $\rho_0 \sim 10^{-9} \text{ Mpc}^{-3} \text{ yr}^{-1}$  [20], whereas the duration is about  $\Delta T \sim 10 - 100 \text{ s}$ . Thus, we have  $n_0 \sim 10^{-15} \text{ Mpc}^{-3}$  and  $\mathcal{N}_\Gamma \sim 10^{-9} (\xi_{\text{CR}}/10)(\Gamma/300)^2 \text{ Mpc}^{-3}$ . The comoving luminosity is  $L'_\gamma \sim 10^{46} - 10^{47} (\Gamma/300)^{-2} \text{ erg s}^{-1}$ . Thus, the high-luminosity GRBs can satisfy the requirement for the unified scenario. However, there is an important caveat in the models. Stacking analyses performed by the IceCube Collaboration show that high-luminosity GRBs can only contribute to  $\lesssim 1\%$  of the diffuse IceCube neutrino flux at least for prompt neutrino emission [21].

Low-luminosity GRBs have been suggested as the origin of UHECRs [22] and some of the theoretical predictions for neutrino emission are consistent with the diffuse neutrino flux measured in IceCube. The common explanation for IceCube neutrinos and UHECRs has also been suggested [24]. The rate density is  $\rho_0 \sim 10^{-7} - 10^{-6} \text{ Mpc}^{-3} \text{ yr}^{-1}$  but with large uncertainty, and the duration is  $\Delta T \sim 1000 - 10000 \text{ s}$ . Thus we expect  $n_0 \sim 10^{-11} \text{ Mpc}^{-3}$  and  $\mathcal{N}_\Gamma \sim 10^{-9} (\xi_{\text{CR}}/10)(\Gamma/3)^2 \text{ Mpc}^{-3}$ . The comoving luminosity is expected to be  $L'_\gamma \sim 10^{46} - 10^{47} (\Gamma/3)^{-2} \text{ erg s}^{-1}$ , and neither stacking analyses nor multiplet limits are strong enough to critically constrain the model. Thus, we conclude that low-luminosity GRBs provide a viable example of the unification scenario, which is consistent with the results of Ref. [25].

Whether the classes of sources discussed above meet the requirements of the unified model is highly dependent on  $\Gamma$  and  $\xi_{\text{CR}}$ . We find that lower values of  $\Gamma$  and/or  $\xi_{\text{CR}}$  than their canonical values are favored to bring more allowed parameter space. The UHECR acceleration power condition, Eq. 3.1, places the most stringent constraints for selecting the possible classes of source candidates. A mixed composition model of UHECRs generally softens this requirement. Relaxing the acceleration condition,  $E_p^{\text{max}} \simeq 2.0 \times 10^{11}$  GeV, makes the scenario of unified UHECR-neutrino scheme more conceivable.

## 6. Summary and Conclusion

We presented a generic model to account both the UHECR and high energy neutrino observations by common sources via  $p\gamma$  interactions. They should be mildly optically thick such as  $0.1 \lesssim \tau_{\gamma p} \lesssim 0.4$  with the energy rate density  $L'_\gamma \mathcal{N}_\Gamma \sim O(10^{37})$  erg s<sup>-1</sup> Mpc<sup>-3</sup>. The magnetic field strength smaller than expected from the equipartition condition, such as  $\xi_B \sim 0.1$ , can enlarge the allowed parameter space. We find that tidal disruption events and low-luminosity GRBs are the most prominent source candidates. The source characteristic parameters like the bulk Lorentz factor  $\Gamma$  and CR loading factor  $\xi_{\text{CR}}$  must be appropriately adjusted, however, to meet all the criteria required by the unified scheme of UHECR-neutrino emissions.

## References

- [1] M. G. Aartsen *et al.* (IceCube Collaboration), Phys. Rev. Lett. **111**, 021103 (2013); M. G. Aartsen *et al.* (IceCube Collaboration), Science **342**, 1242856 (2013); M. G. Aartsen *et al.* (IceCube Collaboration), Phys. Rev. Lett. **113**, 101101 (2014).
- [2] M. G. Aartsen *et al.* (IceCube Collaboration), Astrophys. J. **833**, no. 1, 3 (2016).
- [3] K. Murase and E. Waxman, Phys. Rev. D **94**, 103006 (2016); K. Murase, M. Ahlers, and B. C. Lacki, Phys. Rev. D **88**, 121301(R) (2013); K. Fang and K. Murase, Nature Physics **14**, 396-398 (2018); K. Kachelrieß, *et al.*, Phys. Rev. D **96**, 083006 (2017).
- [4] M. G. Aartsen *et al.* (IceCube Collaboration), Phys. Rev. D **98**, 062003 (2018).
- [5] S. Yoshida and H. Takami, Phys. Rev. D **90**, 123012 (2014).
- [6] M. G. Aartsen *et al.* (IceCube Collaboration), Phys. Rev. Lett. **117**, 241101 (2016); M. G. Aartsen *et al.* (IceCube Collaboration), *ibid.* **119** 259902 (2017)
- [7] The IceCube Collaboration, PoS ICRC2015, 1081 (2015).
- [8] The Pierre Auger Collaboration, PoS ICRC2017, 486 (2017).
- [9] T. Abu-Zayyad *et al.*, Astrophys. J. **768** L1 (2013).
- [10] M. Lemoine and E. Waxman, Journal of Cosmology and Astroparticle Physics, **0911**, 009 (2009).
- [11] E. Waxman and J. Bahcall, Phys. Rev. D **59**, 023002 (1998).
- [12] K. Murase and M. Fukugita, Phys. Rev. D **99**, no. 6, 063012 (2019) doi:10.1103/PhysRevD.99.063012 [arXiv:1806.04194 [astro-ph.HE]].
- [13] M. Ajello *et al.*, Astrophys. J. **780**, 73 (2014) doi:10.1088/0004-637X/780/1/73 [arXiv:1310.0006 [astro-ph.CO]].
- [14] K. Murase, Y. Inoue and C. D. Dermer, Phys. Rev. D **90**, no. 2, 023007 (2014) doi:10.1103/PhysRevD.90.023007 [arXiv:1403.4089 [astro-ph.HE]].
- [15] D. N. Burrows *et al.*, Nature **476**, 421 (2011) doi:10.1038/nature10374 [arXiv:1104.4787 [astro-ph.HE]].
- [16] G. R. Farrar and T. Piran, arXiv:1411.0704 [astro-ph.HE].
- [17] D. Biehl, D. Boncioli, C. Lunardini and W. Winter, Sci. Rep. **8**, no. 1, 10828 (2018) doi:10.1038/s41598-018-29022-4 [arXiv:1711.03555 [astro-ph.HE]].
- [18] N. Senno, K. Murase and P. Meszaros, Astrophys. J. **838**, no. 1, 3 (2017) doi:10.3847/1538-4357/aa6344 [arXiv:1612.00918 [astro-ph.HE]]; C. GuǺlpin, K. Kotera, E. Barausse, K. Fang and K. Murase, Astron. Astrophys. **616**, A179 (2018)
- [19] E. Waxman, Phys. Rev. Lett. **75**, 386 (1995) doi:10.1103/PhysRevLett.75.386 [astro-ph/9505082]. ;M. Vietri, Astrophys. J. **453**, 883 (1995)
- [20] D. Wanderman and T. Piran, Mon. Not. Roy. Astron. Soc. **406**, 1944 (2010) doi:10.1111/j.1365-2966.2010.16787.x [arXiv:0912.0709 [astro-ph.HE]].
- [21] M. G. Aartsen *et al.* [IceCube Collaboration], Astrophys. J. **843**, no. 2, 112 (2017) doi:10.3847/1538-4357/aa7569 [arXiv:1702.06868 [astro-ph.HE]].
- [22] K. Murase, K. Ioka, S. Nagataki and T. Nakamura, Astrophys. J. **651**, L5 (2006) doi:10.1086/509323 [astro-ph/0607104].
- [23] E. Liang, B. Zhang and Z. G. Dai, Astrophys. J. **662**, 1111 (2007) doi:10.1086/517959 [astro-ph/0605200].
- [24] B. T. Zhang, K. Murase, S. S. Kimura, S. Horiuchi and P. MǺl'szǺgros, Phys. Rev. D **97**, no. 8, 083010 (2018) doi:10.1103/PhysRevD.97.083010 [arXiv:1712.09984 [astro-ph.HE]].
- [25] D. Boncioli, D. Biehl and W. Winter, Astrophys. J. **872**, no. 1, 110 (2019) doi:10.3847/1538-4357/aafda7 [arXiv:1808.07481 [astro-ph.HE]].